Biosensors and Bioelectronics 64 (2015) 1–5

Contents lists available at ScienceDirect

Biosensors and Bioelectronics

journal homepage: www.elsevier.com/locate/bios

Short communication

Nanostructured photoelectrochemical biosensor for highly sensitive detection of organophosphorous pesticides

Xinyu Li [a,b], Zhaozhu Zheng [a,b], Xuefeng Liu [c], Shenlong Zhao [a], Shaoqin Liu [a,*]

[a] Key Laboratory of Microsystems and Microstructures Manufacturing, Ministry of Education, Harbin Institute of Technology, Harbin 150080, China
[b] School of Life Science and Technology, Harbin Institute of Technology, Harbin 150080, China
[c] National Center for Nanoscience and Technology, Beijing 100190, China

ARTICLE INFO

Article history:
Received 5 May 2014
Received in revised form
27 July 2014
Accepted 3 August 2014
Available online 11 August 2014

Keywords:
Photoelectrochemical biosensor
Organophosphorus pesticides
AChE
Quantum dots
Graphene

ABSTRACT

A sensitive photoelectrochemical (PEC) biosensor for detection of organophosphorus pesticides (OPs) using the nanocomposite of CdSe@ZnS quantum dots (QDs) and graphene deposited on the ITO coated glass electrode as a photoactive electrode is presented. The integration of CdSe@ZnS/graphene nanocomposite with biomolecules acetylcholinesterase (AChE) as a biorecognition element yields a novel biosensing platform. Under visible light irradiation, the AChE–CdSe@ZnS/graphene nanocomposite can generate a stable photocurrent and the photocurrent is found to be inversely dependent on the concentration of OPs. Under the optimal experimental conditions, the photocurrents were proportional to the logarithm of paraoxon and dichlorvos within the concentration range of 10^{-12}–10^{-6} M. The detection limits (LOD) of the proposed biosensor for paraoxon and dichlorvos are as low as 10^{-14} M and 10^{-12} M. The photoelectrochemical biosensor shows good sensitivity, reproducibility, stability, and could be successfully applied to detection of OPs in real fruit samples.

1. Introduction

The analysis of organophosphates pesticides (OPs) residues is an important concern due to their high toxicity, as well as their ability to accumulate, mobility and long-term effects on living organisms (Patel, 2002; Walker and Asher, 2005). Well-established detection methods for OPs such as gas chromatography, high performance liquid chromatography, gas chromatography–mass spectrometry (GC–MS), and liquid chromatography–mass spectrometry (LC–MS), (Chen and Huang, 2006; Leandro et al., 2006; Rotiroti et al., 2005) offer high sensitivity and selectivity for accurate determination of OP pesticides. However, these methods are cost-intensive, time-consuming and often require well trained technicians and experts to run the analysis.

Compared with the conventional methods, photoelectrochemical (PEC) measurement has attracted considerable interests as a newly developed and promising analytical technique for biological assay (Brown et al., 1992; Chen et al., 2010; Cooper et al., 1998; Tokudome et al., 2005). Owing to the complete separation of excitation source (light) and detection signal (photocurrent), PEC measurements exhibit some advantages of both optical methods and electrochemical sensors, such as low background signals, high sensitivity, inherent miniaturization, portability and easy automation. Recently, the PEC sensing platform for OPs has been reported based on photoactive TiO_2 nanoparticles (Li et al., 2011b). However, current PEC sensing systems face at least three challenges: (1) The wide band gap of TiO_2 only allows it to absorb ultraviolet light ($\lambda < 400$ nm). To extend the photoresponse to the visible region, further modification of TiO_2 with organic dyes (Li et al., 2011a; Tu et al., 2010), inorganic semiconductor nanoparticles (Kang et al., 2010; Zhao et al., 2011) and noble metal nanoparticles (Zhu et al., 2009) has to be done. (2) The photocatalytic oxidation of OPs with TiO_2 gives rise to absence of selectivity. Therefore, how to realize the selectivity of a PEC sensor is an urgent problem to be overcome. Actually, coupling photoactive materials with enzyme (Gong et al., 2012) or molecular imprinted polymers (Li et al., 2013; Shi et al., 2011; Wang et al., 2013) is considered to be beneficial for increasing the selectivity of the photocatalyst. (3) The strong oxidizing power of the photogenerated holes upon illumination may cause the deactivation of biomolecules (Wen et al., 2010; Zou et al., 2001).

Owing to narrower band gap and strong absorption in the visible light region (Ellingson et al., 2005), semiconductor nanoparticles or quantum dots (QDs) are important materials for solar-energy conversion. Recently, the integration of QDs with DNA (Freeman et al., 2007; Gill et al., 2005; Willner et al., 2001) or proteins (Katz et al., 2006; Pardo-Yissar et al., 2003; Stoll et al., 2006; Yildiz et al., 2008) has been extensively studied for the

* Corresponding author. Tel.: +86 451 86403493; fax: +86 451 86403483.
E-mail address: shaoqinliu@hit.edu.cn (S. Liu).

http://dx.doi.org/10.1016/j.bios.2014.08.006
0956-5663/

development of PEC sensing platforms (Gill et al., 2008). However, the photocurrent generated by QDs-biomolecule hybrids is quite low due to rapid electron–hole recombination. Many works demonstrate that the photoresponse of QDs can be efficiently improved with the presence of conductive polymers (Granot et al., 2004) or metallic nanoparticles (NPs) (Sheeney-Haj-Ichia et al., 2004; Subramanian et al., 2001) or semiconductor nanoparticles (Nasr et al., 1997; Sant and Kamat, 2002; Zaban et al., 2000), which practically act as electron traps to help separate the photogenerated charges and subsequently enhance interfacial charge transfer. Moreover, very high photoelectrical conversion efficiency was achieved when CdS nanoparticles were attached to carbon nanotube-modified gold electrodes (Sheeney-Haj-Ichia et al., 2005). It has been suggested that the conductive carbon nanotube is capable of providing efficient paths for the transport of conduction-band electrons to the electrode.

Graphene, a sp^2-bonded carbon sheet with a thickness of single atom and a tunable band gap, is a good candidate for the collection and transport of photogenerated charges (Guo et al., 2010; Wang et al., 2011; Zhou et al., 2009). Therefore, the organization of assemblies of graphene and semiconductor QDs on electrode might provide a novel structure for improved PEC functions. Herein, we report the assembly of graphene/CdSe@ZnS hybrid systems on indium-doped tin oxide (ITO) coated glass electrode surfaces. The system reveals efficient PEC functions. The graphene/CdSe@ZnS assemblies are further modified with acetylcholine esterase (AChE). The AChE in assemblies catalyzes the hydrolysis of acetylthiocholine to generate thiocholine, which acts as an electron donor for the photogenerated holes in the valence band of the CdSe@ZnS QDs and thus enhances the photocurrent. However, the enhanced photocurrent will be obviously decreased when the enzyme activity is inhibited by OPs. On the basis of the inhibition effect of OPs on the photocurrent of graphene/CdSe@ZnS/AChE, a rapid and reliable visible light-activated PEC approach is developed for detecting OPs. To our knowledge, this is one of the most sensitive PEC biosensors used for OPs detection till now.

2. Materials and methods

2.1. Reagents and materials

Cadmium oxide (CdO, 98.9%), selenium (99%, powder), sulfur (99.9%, powder), 1-octadecene (ODE, 90%), 2-mercaptoethylamine, mercaptopropionic acid (MPA, 99%), AChE (EC 3.1.1.7 from *Electrophorus electricus*, lyophilized, specific activity 435 U/mg), acetylthiocholine chloride, and poly(ethyleneimine) (PEI, MW 25,000) were purchased from Aldrich. Zinc acetate (99%, powder), oleic acid (80%) and trioctylphosphine (90%) were obtained from Acros Organics, Merck and Fluka, respectively. Graphite powder was obtained from Beijing Chemical Reagents Company. The standard samples of paraoxon, dichlorvos (100 μg mL^{-1} in acetone) were purchased from Beijing (Weiyekechuang Keji Co., Ltd., China). Other chemicals of analytical grade were obtained from commercial sources and used as received. All solutions were prepared with ultrapure water from a Milli-Q water purification system (Billerica, MA). The ITO (about 15 Ω/sq) coated glass was obtained from Leaguer Film Technology (Shenzhen).

2.2. Apparatus

The UV–Vis absorption spectra were measured by using a U4100 UV–Vis–NIR spectrometer (Hitachi, Japan), and the fluorescence spectra were recorded with a Fluoromax-4 fluorescence spectrophotometer (Horiba Jobin Yvon, Japan). If not specifically stated, the samples were excited at 380 nm, and the exciting slit and the emission slit were both 5 nm. The optical properties of solutions and the multilayer films were measured using quartz cuvette with 1 cm path length and a standard solid sample holder, respectively. Electrochemical measurements were performed with a 660 series potentiostat (CH Instruments, Austin, USA) with a conventional three electrode system comprising platinum wire as auxiliary electrode, a standard Ag/AgCl in saturated KCl solution as the reference electrode, and as-prepared graphene/CdSe@ZnS or graphene/CdSe@ZnS/AChE electrode as the working electrode. During the electrochemical measurements, the electroactive surface area of the working electrode was ca. 3.8 cm^2. A 150 W xenon lamp (CROWNTECH, USA) equipped with a filter was used as the irradiation source ($\lambda > 400$ nm).

2.3. Fabrication of the proposed biosensor preparation of graphene/CdSe@ZnS/AChE hybrid modified electrode

An aqueous dispersion of fewer-layered graphene was prepared from pristine graphite according to the modified Hummers method (Li et al., 2008) and the thickness of graphene is approximately 1.51 nm (Fig. S1). MPA-capped CdSe@ZnS QDs with fluorescence peaks at 630 nm were synthesized according to the previous method (Wang et al., 2007). The average particle sizes were estimated to be 5.5 nm (Fig. S2) and the concentration was about 10^{-6} M.

Prior to the preparation of graphene/CdSe@ZnS/AChE electrodes, the bare ITO substrates were cleaned according to a literature procedure (Evenson et al., 1996). Before assembly, the cleaned ITO-coated glass electrodes were functionalized with (3-aminopropyl) trimethoxysilane to yield an amine-functionalized surface. As illustrated in Fig. S3, the $(graphene/PEI/QDs/PEI)_x$ films were alternatively deposited from the prepared graphene solution, 10^{-6} M MPA-capped CdSe@ZnS QDs and 1 mg/mL PEI solution, using an immersion time of 10 min, and then rinsed with pure water and dried under N_2 flow after each layer deposited. AChE enzyme immobilization was achieved by alternatively immersing the obtained $(graphene/PEI/QDs/PEI)_x$ films in 20 mM phosphate buffer (pH 7.0) containing 0.5 mg/mL of AChE and 1 mg/mL PEI (pH 6.0) for 10 min. The resulting graphene/CdSe@ZnS/AChE electrode was stored at −20 °C for use.

2.4. PEC biosensing under visible light illumination

For the measurements of paraoxon and dichlorvos as the model of OPs, the obtained graphene/CdSe@ZnS/AChE electrode was first immersed in phosphate buffer solution (PBS, 0.1 M, pH 7.4) containing different concentrations of standard OPs at 37 °C for 15 min, and then 1.5 mM acetylthiocholine, an enzyme substrate, was added to above solution to study the PEC response. For comparison, the PEC responses were also recorded by immersing the graphene/CdSe@ZnS/AChE electrode in a solution of 1.5 mM acetylthiocholine for 15 min in the absence of OPs. The inhibition of OPs was calculated as follows:

$$\text{Inhibition}(\%) = (I_{without} - I_{with})/I_{without} \times 100$$

where $I_{without}$ and I_{with} were the photocurrent of acetylthiocholine on the graphene/CdSe@ZnS/AChE electrode, in the absence and presence of OP inhibition, respectively.

2.5. Preparation and detection of fruit samples

The procedure for OP determination in real samples was as follows: (1) The fruit sample was first chopped by a steel automatic vegetable fruit chopper machine and extracted with 20 mL PBS solution, then centrifugation at 3000 rpm for 10 min. (2) The

biosensor was incubated with the extracted solution at 37 °C for 15 min. (3) After being rinsed with PBS and dried under N_2 flow, the PEC response was measured in 3 mL PBS solution with 1.5 mM acetylthiocholine. The inhibition percentages of different samples were compared with the calibration curve, and then the OP concentration in the real sample could be obtained.

3. Results and discussion

3.1. Fabrication and PEC properties of graphene/CdSe@ZnS QDs hybrid film

As illustrated in Fig. S3, we used layer-by-layer assembly technique for fabrication of graphene/QDs/AChE nanocomposite film. Because graphene, MPA-capped CdSe@ZnS QDs and AChE are negatively charged, the positively charged PEI must be introduced to offer the opposite charge for immobilizing graphene, MPA-capped CdSe@ZnS QDs and AChE sequentially on the ITO substrate. The assembly of graphene and MPA-capped CdSe@ZnS QDs on the quartz substrates is characterized by the UV–Vis spectra (Fig. S4a). Both the absorbance shoulders at 611 nm ($\lambda_{611\ nm}$) (Fig. S4b) and 270 nm (Fig. S4c) of (graphene/PEI/CdSe@ZnS/PEI)$_x$ linearly increase with the number of bilayers, x, which confirms irreversible adsorption of CdSe@CdS QDs and graphene on the substrate. The incorporation of graphene in the hybrid is also confirmed by Raman measurements. Raman spectrum of hybrid films (Fig. S5) displays the characteristic peaks of the D band (disorder band caused by the graphite edges) and G band (in-phase vibration band of graphite lattice) at 1351 and 1595 cm^{-1}, respectively (Kudin et al., 2008).

The PEC properties of (graphene/PEI/CdSe@ZnS/PEI)$_4$ functionalized ITO electrodes were examined in 0.1 M PBS (pH 7.4). The resulting photocurrent responses are shown in Fig. S6a. In the dark, the *I–V* curve shows typically rectifying behavior. Under illumination, the photocurrent density increases 2-fold compared to that in the dark. The corresponding photocurrent response to ON–OFF cycles is presented in the insert of Fig. S6a. Under illumination, the (graphene/PEI/CdSe@ZnS/PEI)$_4$ functionalized ITO electrode reaches over 129% of the steady-state current within 1 s. When the light source is turned off, the system immediately returns to its initial state. That is, a steady and prompt photocurrent generation is obtained during on and off cycles of illumination. In a control experiment, no photocurrent is observed upon irradiation of graphene-functionalized electrode that lacks the CdSe@ZnS NPs (red curve in Fig. S6b). This result indicates that the photocurrent originates from the CdSe@ZnS NPs and that the graphene is not photoactive. In another control experiment, four CdSe@ZnS/PEI bilayers are assembled on an ITO electrode. It can be found that the photocurrent generated by (CdSe@ZnS/PEI)$_4$ (green curve in Fig. S6b) and (graphene/PEI/CdSe@ZnS/PEI)$_4$ functionalized electrode (blue curve in Fig. S6b) is 2.07 μA and 3.92 μA at a bias voltage of 0.2 V, respectively. Evidently, the photocurrent generated by the system that lacks the graphene is much lower. Thus, we conclude that graphene play a major role in the enhanced generation of photocurrent.

We further examined the effect of the layer number of graphene/PEI/CdSe@ZnS/PEI hybrid film on the resulting photocurrent. The obtained photocurrents reveal that the photocurrent is enhanced as the number of the graphene/PEI/CdSe@ZnS/PEI layer increases (Fig. 1a). The photocurrent increases from 3.92 μA of 4 layers, to 6.97 μA of 7 layers, and to 10.12 μA of 10 layers of graphene/PEI/CdSe@ZnS/PEI at 0.2 V. However, the photocurrent of CdSe@ZnS/PEI hybrid film only increased from 2.07 μA of 4 bilayers to 7.67 μA of 10 bilayers. The results clearly demonstrate the very efficient generation of photocurrent in the graphene/CdSe@ZnS hybrid film. The improved photoconversion efficiency is mainly attributed to the unique abilities of graphene to efficiently separate the photogenerated carriers and consequently hinder the recombination of electrons and holes in QDs (Dong et al., 2012; Du et al., 2011, 2012; Q. Li et al., 2011; Long et al., 2012).

3.2. PEC behavior of graphene/CdSe@ZnS/AChE QDs hybrid film

AChE enzymes were further assembled on the graphene/CdSe@ZnS hybrid film. In comparison to the graphene/CdSe@ZnS hybrid film modified electrode, with introduction of AChE onto graphene/CdSe@ZnS hybrid film, the photocurrent of graphene/CdSe@ZnS/AChE functionalized ITO electrode is reduced (Fig. S7) most likely because the thicker enzyme film may block charge transfer across the interface between graphene/CdSe@ZnS hybrid film and electrolyte. Further addition of acetylthiocholine, an enzyme substrate, to PBS solution results in a significantly enhanced photocurrent in the graphene/CdSe@ZnS/AChE hybrid system (red curve in Fig. 1b). For example, upon addition of 1.5 mM acetylthiocholine, the photocurrent of (graphene/PEI/QDs/PEI)$_4$(AChE/PEI)$_4$ modified ITO electrode increases by 4.42 μA, which is 2.2 times compared with the photocurrent increment of 2.02 μA observed in the absence of acetylthiocholine (black curve in Fig. 1b). In a control experiment, no obvious photocurrent enhancement is observed upon irradiation of graphene/CdSe@ZnS functionalized electrode in the presence of

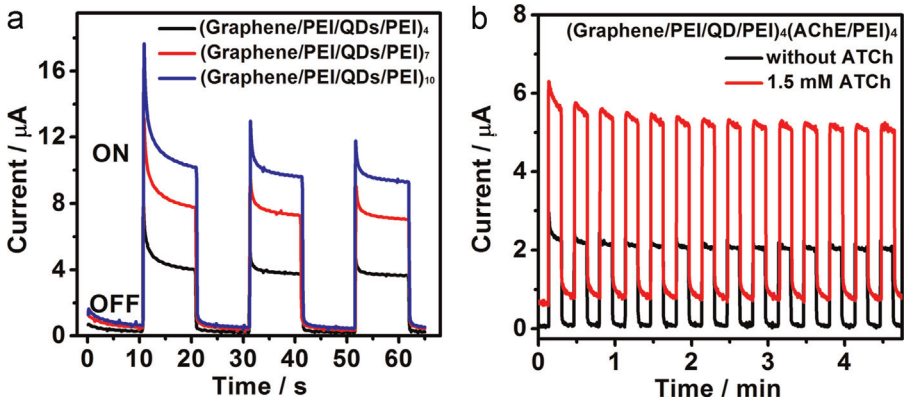

Fig. 1. (a) Dependence of photocurrent on the layer number of graphene/PEI/CdSe@ZnS/PEI hybrids. Photocurrent responses were recorded in 100 mM PBS, pH 7.4 under visible light. (b) Photocurrent responses of (graphene/PEI/QDs/PEI)$_4$(AChE/PEI)$_4$ before (black) and after (red) addition of 1.5 mM acetylthiocholine. Photocurrent responses were recorded in 100 mM PBS, pH 7.4 under visible light. (For interpretation of the references to color in this figure legend, the reader is referred to the web version of this article.).

acetylthiocholine. Therefore, on the basis of above phenomenon, the photocurrent enhancement after addition of enzyme substrate could be attributed to the AChE-catalyzed hydrolysis of acetylthiocholine to acetate and thiocholine. As shown in the band diagram of graphene/CdSe@ZnS and thiocholine (Fig. S8), it is clear that the redox potential of thiocholine lies above the valence band of CdSe@ZnS. Upon irradiation, the latter product, thiocholine acts as a sacrificial electron donor for the photogenerated holes in the valence band of the CdSe@ZnS NPs, and thus improves the efficiency of charge separation, leading to a prominent increase in the photocurrent.

OPs could attack the active center of the enzyme AChE and reduce the enzymatic activity to the substrate, leading to the decrease in the thiocholine production. Thus, the photocurrent response of graphene/CdSe@ZnS/AChE functionalized electrode is also investigated by incubated in the OP solution for 15 min. The photocurrent–time curves of $(graphene/PEI/QDs/PEI)_4(AChE/PEI)_4$ functionalized electrode clearly illustrate that after incubation with different concentration paraoxon (as the typical compound of OPs), the photocurrents in $(graphene/PEI/QDs/PEI)_4(AChE/PEI)_4$ functionalized electrode decrease (Fig. 2a). Due to the notable change in PEC signal of the graphene/CdSe@ZnS/AChE hybrid system, the graphene/CdSe@ZnS/AChE functionalized electrode could be used for PEC biosensing of OPs under visible light irradiation.

3.3. PEC detection of OPs by the graphene/QDs/AChE hybrid modified ITO electrode

Since the proposed method for the determination of OPs is based on the change in PEC signal of the graphene/CdSe@ZnS/AChE hybrid system, the effect factors for measurements concerning enzyme loading, substrate, pH of buffer solution, reaction temperature and incubation time with OPs were studied in detail (see detailed discussion in Part S3, Figs. S9, S10 and S11). In summary, the optimal conditions for the deterimation of OPs are the $(graphene/PEI/QDs/PEI)_4(AChE/PEI)_4$ functionalized electrode, 1.5 mM acetylthiocholine, pH7.4, 37 °C and incubation time of 15 min.

Under the optimized experimental conditions, the detection of two typical OPs, paraoxon and dichlorvos was performed using the $(graphene/PEI/QDs/PEI)_4(AChE/PEI)_4$ functionalized electrode. As shown in Fig. 2b and c, the paraoxon inhibition to $(graphene/PEI/QDs/PEI)_4(AChE/PEI)_4$ functionalized electrode is proportional to the logarithm of paraoxon and dichlorvos within the concentration range of 10^{-12} M to 10^{-6} M. The regression equation is inhibition (%) = 1.30 + 0.10 log [dichlorvos] (R^2 = 0.993, n = 6) for dichlorvos and inhibition (%) = 1.56 + +0.11 log [paraoxon] (R^2 = 0.975, n = 6) for paraoxon, respectively. The detection limit (LOD) is set to be the concentration of OP that causes 10% inhibition (Skladal et al., 1997). It is worth mentioning that the calculated detection limit is as low as about 2.5×10^{-12} M for dichlorvos and 6.0×10^{-14} M for paraoxon. The detection limit obtained is significantly lower than that reported so far with an enzyme-based inhibitor electrochemical sensor (see Table S1 in Supplementary Information).

The analytical reliability of this PEC sensor was evaluated by assaying same concentration of paraoxon and dichlorvos with six electrodes made by the same procedures independently. The relative standard deviation (RSD) among six detection of the same concentration of OPs is found to be less than 15%, indicating an acceptable reproducibility. The stability of the $(graphene/PEI/QDs/PEI)_4(AChE/PEI)_4$ functionalized electrode is also examined after 60 day storage at −20 °C. The identical measurement results highlight that the biosensors could retain all the enzyme activity and show good stability even after 6 months (Fig. S11). The interferences from 100-fold heavy metal ions (Cu^{2+}, Cd^{2+}, Hg^{2+}, Pb^{2+} and Zn^{2+}) were examined. The obvious inhibition behavior can also be observed (Fig. S12). However, the percentages of inhibition are less than 30% for 10^{-7} M heavy metal ions, which are considerably smaller than those of 10^{-9} M dichlorvos (39.6 ± 4.1%) and paraoxon (52.7 ± 3.4%). This result demonstrates that the proposed biosensor could be used for the detection of low concentration of OPs.

3.4. Analysis of pesticide in real samples

To demonstrate the feasibility of the sensors applied to practical samples, the determination of paraoxon and dichlorvos in real fruit samples was performed. We perform the recovery tests by adding different amounts of OP into apple samples, and the results are summarized in Table 1. The original inhibition rate in the apple sample was tested to be 4.80 ± 1.41%, well below 10%, so we assume that OP residue is not detected. The recoveries of the spiked OPs are from 93.6 ± 12.1% to 103.3 ± 12.8%. The results obtained by the above method also accord very well with those by HPLC–MS, which disclose that the nanostructured biosensors are capable of practical application.

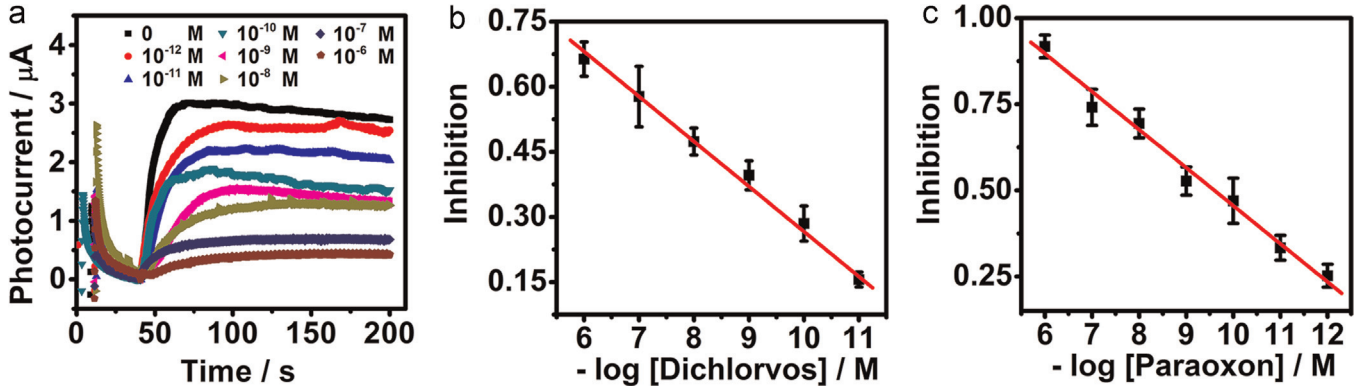

Fig. 2. (a) Photocurrent responses of $(graphene/PEI/QDs/PEI)_4(AChE/PEI)_4$ functionalized electrode toward 1.5 mM acetylthiocholine under visible light after incubation with 0, 10^{-12}, 10^{-11}, 10^{-10}, 10^{-9}, 10^{-8}, 10^{-7} and 10^{-6} M (from top to bottom) paraoxon solution, respectively. Calibration curves for the PEC determination of dichlorvos (b) and paraoxon (c) at $(graphene/PEI/QDs/PEI)_4(AChE/PEI)_4$ functionalized electrode. Each data point is an average of six measurements. The correlation coefficients are 0.993 and 0.975, respectively. All experiments were measured in 100 mM PBS (pH 7.4, 37 °C) containing 1.5 mM acetylthiocholine. The applied potential was 0.2 V vs Ag/AgCl (Sat. KCl) upon irradiation with a xenon light source.

Table 1
Recovery ratios of OPs in real fruit samples.

Sample	Spiked	Experimental value (*I*%)	Average value	Recovery (%)	UPLC–MS	Recovery (%)
Apple	0	4.80 ± 1.41	N/A[a]	–	N/A[b]	–
Apple, added paraoxon	10 nM	67.55 ± 0.64	9.93 ± 1.31 nM RSD = 13.19%	99.3 ± 13.1	9.70 ± 0.23	97.0 ± 2.3
Apple, added paraoxon	10 pM	34.61 ± 0.63	10.31 ± 1.28 pM RSD = 12.39%	103.3 ± 12.8	N/A[b]	–
Apple, added dichlorvos	10 nM	47.05 ± 0.58	9.36 ± 1.21 nM RSD = 12.97%	93.6 ± 12.1	9.35 ± 0.36	93.5 ± 3.6
Apple, added dichlorvos	10 pM	16.07 ± 0.50	9.65 ± 1.1 pM RSD = 11.40%	96.5 ± 11.0	N/A[b]	–

[a] Since the inhibition rate is lower than 10%, we assume that OP residue is not detected.
[b] Total OP content in natural vegetable and fruit samples is lower than the limit of detection by UPLC–MS, so the OPs cannot be detected out.

4. Conclusion

In this study, a novel PEC biosensing platform is constructed by using QD/graphene hybrid system. Upon visible light irradiation, the QD/graphene hybrid system exhibits improved photocurrent responses. The improved photoelectric conversion efficiency is mainly attributed to the unique abilities of graphene to efficiently separate the photogenerated carriers and consequently hinder the recombination of electrons and holes in QDs. The integration of QD/graphene hybrid system with AChE biomolecules yields a highly sensitive PEC assays for OPs. The resulting biosensor shows many unique advantages such as low bias voltage, rapid response, excellent sensitivity, good reproducibility, ideal stability and fine applicability for the detection of OPs in real samples. The good performance, simple and inexpensive fabrication and easy to use endow these nanostructured biosensors great potentials for practical application. This strategy not only extends the application of pesticides, but also presents a simple, economic and novel methodology for PEC sensing of important chemical or biological species. However, it should be noted that there is potential toxicity for use of CdSe@ZnS QDs as the components of the biosensors, therefore in the future work the low-toxic QDs like ZnSe or Ag_2Se will be attempted.

Acknowledgments

The authors acknowledge support from the National Natural Science Foundation of China (Grant nos. 20773033 and 91023007) and Outstanding Young Funding of Heilongjiang Province.

Appendix A. Supplementary information

Supplementary information associated with this article can be found in the online version at http://dx.doi.org/10.1016/j.bios.2014.08.006.

References

Brown, G.N., Birks, J.W., Koval, C.A., 1992. Anal. Chem. 64, 427–434.
Chen, D., Zhang, H., Li, X., Li, J., 2010. Anal. Chem. 82, 2253–2261.
Chen, P.S., Huang, S.D., 2006. Talanta 69, 669–675.
Cooper, J.A., Wu, M., Compton, R.G., 1998. Anal. Chem. 70, 2922–2927.
Dong, C., Li, X., Jin, P., Zhao, W., Chu, J., Qi, J., 2012. J. Phys. Chem. C 116, 15833–15838.
Du, A., Ng, Y.H., Bell, N.J., Zhu, Z., Amal, R., Smith, S.C., 2011. J. Phys. Chem. Lett. 2, 894–899.
Du, A., Sanvito, S., Li, Z., Wang, D., Jiao, Y., Liao, T., Sun, Q., Ng, Y.H., Zhu, Z., Amal, R., Smith, S.C., 2012. J. Am. Chem. Soc. 134, 4393–4397.
Ellingson, R.J., Beard, M.C., Johnson, J.C., Yu, P.R., Micic, O.I., Nozik, A.J., Shabaev, A., Efros, A.L., 2005. Nano Lett. 5, 865–871.
Evenson, S.A., Badyal, J.P.S., Pearson, C., Petty, M.C., 1996. J. Phys. Chem. 100, 11672–11674.
Freeman, R., Gill, R., Beissenhirtz, M., Willner, I., 2007. Photochem. Photobiol. Sci. 6, 416–422.
Gill, R., Patolsky, F., Katz, E., Willner, I., 2005. Angew. Chem. Int. Ed. 44, 4554–4557.
Gill, R., Zayats, M., Willner, I., 2008. Angew. Chem. Int. Ed. 47, 7602–7625.
Gong, J., Wang, X., Li, X., Wang, K., 2012. Biosens. Bioelectron. 38, 43–49.
Granot, E., Patolsky, F., Willner, I., 2004. J. Phys. Chem. B 108, 5875–5881.
Guo, C.X., Yang, H.B., Sheng, Z.M., Lu, Z.S., Song, Q.L., Li, C.M., 2010. Angew. Chem. Int. Ed. 49, 3014–3017.
Kang, Q., Yang, L.X., Chen, Y.F., Luo, S.L., Wen, L.F., Cai, Q.Y., Yao, S.Z., 2010. Anal. Chem. 82, 9749–9754.
Katz, E., Zayats, M., Willner, I., Lisdat, F., 2006. Chem. Commun. 7, 1395–1397.
Kudin, K.N., Ozbas, B., Schniepp, H.C., Prud'homme, R.K., Aksay, I.A., Car, R., 2008. Nano Lett. 8, 36–41.
Leandro, C.C., Hancock, P., Fussell, R.J., Keely, B.J., 2006. J. Chromatogr. A 1103, 94–101.
Li, D., Muller, M.B., Gilje, S., Kaner, R.B., Wallace, G.G., 2008. Nat. Nanotechnol. 3, 101–105.
Li, H.B., Li, J., Xu, Q., Hu, X.Y., 2011a. Anal. Chem. 83, 9681–9686.
Li, H.B., Li, J., Xu, Q., Yang, Z.J., Hu, X., 2013. Anal. Chem. Acta 766, 47–52.
Li, H.B., Li, J., Yang, Z.J., Xu, Q., Hu, X.Y., 2011b. Anal. Chem. 83, 5290–5295.
Li, Q., Guo, B., Yu, J., Ran, J., Zhang, B., Yan, H., Gong, J.R., 2011. J. Am. Chem. Soc. 133, 10878–10884.
Long, R., English, N.J., Prezhdo, O.V., 2012. J. Am. Chem. Soc. 134, 14238–14248.
Nasr, C., Hotchandani, S., Kim, W.Y., Schmehl, R.H., Kamat, P.V., 1997. J. Phys. Chem. B 101, 7480–7487.
Pardo-Yissar, V., Katz, E., Wasserman, J., Willner, I., 2003. J. Am. Chem. Soc. 125, 622–623.
Patel, P.D., 2002. Trends Anal. Chem. 21, 96–115.
Rotiroti, L., Stefano, L.D., Rendina, I., Moretti, L., Rossi, A.M., Piccolo, A., 2005. Biosens. Bioelectron. 20, 2136–2139.
Sant, P.A., Kamat, P.V., 2002. Phys. Chem. Chem. Phys. 4, 198–203.
Sheeney-Haj-Ichia, L., Basnar, B., Willner, I., 2005. Angew. Chem. Int. Ed. 44, 78–83.
Sheeney-Haj-Ichia, L., Pogorelova, S., Gofer, Y., Willner, I., 2004. Adv. Funct. Mater. 14, 416–424.
Shi, H., Zhao, G., Liu, M., Zhu, Z., 2011. Electrochem. Commun. 13, 1404–1407.
Skladal, P., Nunes, G.S., Yamanaka, H., Ribeiro, M.L., 1997. Electroanalysis 9, 1083–1087.
Stoll, C., Kudera, S., Parak, W.J., Lisdat, F., 2006. Small 2, 741–743.
Subramanian, V., Wolf, E., Kamat, P.V., 2001. J. Phys. Chem. B 105, 11439–11446.
Tokudome, H., Yamada, Y., Sonezaki, S., Ishikawa, H., Bekki, M., Kanehira, K., Miyauchi, M., 2005. Appl. Phys. Lett. 87, 213901–213903.
Tu, W.W., Dong, Y.T., Lei, J.P., Ju, H.X., 2010. Anal. Chem. 82, 8711–8716.
Walker, J.P., Asher, S.A., 2005. Cryst. Anal. Chem. 77, 1596–1600.
Wang, P.P., Dai, W.J., Ge, L., Yan, M., Ge, S.G., Yu, J.H., 2013. Analyst 138, 939–945.
Wang, Q.B., Xu, Y., Zhao, X.H., Chang, Y., Liu, Y., Jiang, L.J., Sharma, J., Seo, D.K., Yan, H., 2007. J. Am. Chem. Soc. 129, 6380–6381.
Wang, X., Wang, J.F., Cheng, H.J., Yu, P., Ye, J.S., Mao, L.Q., 2011. Langmuir 27, 11180–11186.
Wen, D., Guo, S.J., Wang, Y.Z., Dong, S.J., 2010. Langmuir 26, 11401–11406.
Willner, I., Patolsky, F., Wasserman, J., 2001. Angew. Chem. Int. Ed. 40, 1861–1864.
Yildiz, H.B., Freeman, R., Gill, R., Willner, B., 2008. Anal. Chem. 80, 2811–2816.
Zaban, A., Chen, S.G., Chappel, S., Gregg, B.A., 2000. Chem. Commun., 2231–2232.
Zhao, W.W., Yu, P.P., Xu, J.J., Chen, H.Y., 2011. Electrochem. Commun. 13, 495–497.
Zhou, M., Zhai, Y.M., Dong, S.J., 2009. Anal. Chem. 81, 5603–5613.
Zhu, W., An, Y.R., Luo, X.M., Wang, F., Zheng, J.H., Tang, L.L., Wang, Q.J., Zhang, Z.H., Zhang, W., Jin, L.T., 2009. Chem. Commun. 19, 2682–2684.
Zou, Z.G., Ye, J.H., Sayama, K., Arakawa, H., 2001. Nature 414, 625–627.